THE UNIVERSITY of EDINBURGH

Edinburgh Research Explorer

Internal drainage has sustained lowrelief Tibetan landscapes since the early Miocene

Citation for published version:
Han, Z, Sinclair, HD, Li, Y, Wang, C, Tao, Z, Qian, X, Ning, Z, Zhang, J, Wen, Y, Lin, J, Zhang, B, Xu, M, Dai, J, Zhou, A, Liang, H & Cao, S 2019, 'Internal drainage has sustained lowrelief Tibetan landscapes since the early Miocene', *Geophysical Research Letters*. https://doi.org/10.1029/2019GL083019

Digital Object Identifier (DOI):
10.1029/2019GL083019

Link:
Link to publication record in Edinburgh Research Explorer

Document Version:
Peer reviewed version

Published In:
Geophysical Research Letters

Publisher Rights Statement:
© 2019 American Geophysical Union. All rights reserved.

General rights
Copyright for the publications made accessible via the Edinburgh Research Explorer is retained by the author(s) and / or other copyright owners and it is a condition of accessing these publications that users recognise and abide by the legal requirements associated with these rights.

Take down policy
The University of Edinburgh has made every reasonable effort to ensure that Edinburgh Research Explorer content complies with UK legislation. If you believe that the public display of this file breaches copyright please contact openaccess@ed.ac.uk providing details, and we will remove access to the work immediately and investigate your claim.

OPEN ACCESS

Download date: 28. Aug. 2022

Li Yalin (Orcid ID: 0000-0002-9757-9092)
Wang Chengshan (Orcid ID: 0000-0002-7403-0582)
Dai Jingen (Orcid ID: 0000-0002-6230-6801)

Internal drainage has sustained low-relief Tibetan landscapes since the early Miocene

Zhongpeng Han[1,2], Hugh D. Sinclair[3], Yalin Li[1,2]*, Chengshan Wang[1,2], Zui Tao[3], Xinyu Qian[1,2], Zijie Ning[1,2], Jiawei Zhang[1,2], Yixiong Wen[1,2], Jie Lin[1,2], Baosen Zhang[1,2], Ming Xu[1,2], Jingen Dai[1,2], Aorigele Zhou[1,2], Huimin Liang[4], Shuo Cao[1,2]

[1]State Key Laboratory of Biogeology and Environment Geology, China University of Geosciences, Beijing 100083, China

[2]School of Earth Sciences and Resources, China University of Geosciences, Beijing 100083, China

[3]School of GeoSciences, The University of Edinburgh, Drummond Street, Edinburgh, EH8 9XP, UK

[4]Chengdu Center, China Geological Survey, Chengdu 610081, China

*Corresponding author: Yalin Li (liyalin@cugb.edu.cn)

Key words: central Tibet; Lunpola Basin; internal drainage; early Miocene; low-relief; paleogeography

Key Points:

- Robust age constraints of the youngest continental stratigraphic unit from the Lunpola Basin in central Tibet are reported.
- Aggradation and erosion of internal drainage dominated the formation of low-relief topography in central Tibet by the early Miocene times.
- Late Cenozoic drainage basins in central Tibet developed in response to flow in the lower crust and/or mantle lithosphere.

This article has been accepted for publication and undergone full peer review but has not been through the copyediting, typesetting, pagination and proofreading process which may lead to differences between this version and the Version of Record. Please cite this article as doi: 10.1029/2019GL083019

© 2019 American Geophysical Union. All rights reserved.

Accepted Article

Abstract

The timing of formation of the low-gradient, internally drained landscape of the Tibetan Plateau is fundamental to understanding the evolution of the plateau as a whole. Well-dated sedimentary records of internal drainage of rivers into lakes are used to reveal the timing of this evolution. Here, we redate the youngest continental sedimentary successions of central Tibet in the Lunpola Basin and propose a new age range of ca. 35 to 9 Ma, significantly younger than previously thought. We demonstrate long-standing internal drainage in central Tibet since the late Eocene and stable sedimentary environments, source regions, and low topographic relief since at least the early Miocene. We suggest that sediment aggradation of internal drainage and reduction of hillslope gradients by erosion dominate the formation of low-relief landscapes and that the late Cenozoic drainage basins in central Tibet developed in response to flow in the lower crust and/or mantle lithosphere.

Plain Language Summary

Internal drainage of rivers into lakes is a characteristic of the high plateaus of the world and, most notably, the Tibetan Plateau. Internal drainage generates local perched base-levels for Tibetan rivers, enabling geomorphic isolation from the rapidly incising rivers of the Himalaya and surrounding regions. However, the question of when the low-relief plateau topography was initiated has been largely ignored, and its formation mechanism is controversial. Here, we report a detailed investigation in the Lunpola Basin of central Tibet and propose a new depositional age range of ca. 35-9 Ma. We demonstrate that the internal drainage kept eroding the mountain ranges and filling the surrounding lowlands since at least the late Eocene. By no later than the early Miocene, a gentle landscape formed in central Tibet. The late Cenozoic basins in central Tibet developed in response to deep crustal or mantle flow and associated upper crustal deformation.

Accepted Article

© 2019 American Geophysical Union. All rights reserved.

1 Introduction

The modern-day internally drained hinterland of the Tibetan Plateau has a relatively low-relief topography, in stark contrast to the high-relief externally drained Himalaya and surrounding mountain ranges (Fielding et al., 1994; Figure 1a). As the largest orogenic plateau, the evolution of this striking geomorphic feature is crucial for understanding the earth's surface and underlying dynamic processes. While there has been extensive discussion of the temporal and spatial evolution of the plateau, the timing and mechanism of development of the low-relief topography remain a challenge (Clark and Royden, 2000; Liu-Zeng et al., 2008). The isolation of elevated river base-levels as a result of rivers terminating in lakes within the interior plateau is a requirement for maintaining low-relief topography through sediment aggradation of river channels and reduction in hillslope gradients by weathering and erosion (Liu-Zeng et al., 2008). Detailed dating of the sedimentary successions that record internal drainage is essential for understanding the plateau's evolution. However, few studies have tested the geological evidence for the longevity of internal drainage in central Tibet and, hence, for the low-relief topography.

Cenozoic continental sediments are preserved in several basins along the Bangong-Nujiang suture of central Tibet, which experienced large-scale upper crustal shortening and thickening during the Late Cretaceous to Paleogene (Kapp et al., 2005). The present deformation pattern of central Tibet is dominated by north-south oriented extensional structures, with northeast-striking left-slip faults and northwest-striking right-slip faults (Royden et al., 2008). These strike-slip faults exert key control on the elongated geometry of Cenozoic basins such as the Lunpola and Nima Basins, which record the evolution of paleoenvironments and sediment routing in central Tibet (Taylor et al., 2003).

Here, we present our field observations from the Lunpola Basin, apply geochronological, sedimentological and provenance techniques to establish the stratigraphic

Accepted Article

© 2019 American Geophysical Union. All rights reserved.

framework and reconstruct depositional systems and drainage networks, and then compare these results with the modern drainage of central Tibet. Our newly dated continental sedimentary successions of central Tibet are significantly younger than previously thought, thus providing new insights into the basin evolution and the formation of the low-relief landscape that characterizes the plateau.

2. Geological background

The Lunpola Basin and adjacent Nima Basin are the two largest Cenozoic basins in central Tibet, and between them is the largest saline lake of Tibet, Silin Co (Figure 1b). The two largest interior rivers of Tibet (Zhajia Zangbo and Bocang Zangbo) originate in the Qiangtang and Lhasa terranes and terminate in the Lunpola-Silin Co-Nima area (Figure 1b). The Bangong-Nujiang suture separates the Qiangtang and Lhasa terranes; the southern Qiangtang terrane is bounded to the north by the Tanggula Shan Range-Qiangtang Central Uplift, and the Gangdese mountains define the northern Lhasa terrane to the south (Figure 1a; Text S1).

More than 4 km thick Cenozoic fluvial to lacustrine deposits in the Lunpola Basin unconformably overly the Mesozoic basement, which were divided into the Paleocene to Eocene Niubao Formation and Oligocene to early Miocene Dingqinghu Formation in previous studies (Wei et al., 2017). Sun et al (2014) proposed a succession of the Dingqinghu Formation ranges from 25.5 to 19.8 Ma based on a single magnetostratigraphic section supported by biostratigraphy and dating of the bentonite layer (He et al., 2012). A mammalian fossil with an age of 18 to 16 Ma was used to define the age of the deep lake deposits of the Dingqinghu Formation in the basin center (Deng et al., 2012), and a tuff layer with an age of 20.6 Ma was found below the mammalian fossil (Mao et al., 2019). However, despite the above constraints, most of the outcrops were assigned a broad age range of Paleocene to Oligocene based on fossil ostracods and palynological assemblages (Xia and

© 2019 American Geophysical Union. All rights reserved.

Accepted Article

Liu, 2008). Thus, the precise depositional ages of these sediments remain uncertain, and stratigraphic correlations with more robust constraints are required.

3. Methods

Sixteen stratigraphic sections of Cenozoic deposits were measured in the Lunpola Basin (Figure 1c). The stratigraphic framework is established by zircon U-Pb ages, facies correlation analyses, fossil-bearing beds, and lateral correlation of outcrops in the field (Figures 2, 3, and S1). Paleocurrent directions were acquired from the entire succession from planar and trough cross-bedding, current ripple lamination, imbricated clasts in conglomerates and sole marks on beds. Point-counting was performed on 92 petrographic thin sections according to the Gazzi-Dickinson method (Ingersoll et al., 1984). Approximately 400 grains were counted in each thin section, and the data were plotted on standard Ternary diagrams with provenance fields established after Dickinson and Suczek (1979). Compositions of conglomerate and modern river gravels were determined by point-counting lithology from measured sections and riverbeds in the Lunpola-Silin Co-Nima area. To ensure that all the counting data are statistically significant and comparable, all countings were performed on the channelized sediments. Fifteen sandstone and tuffite samples were collected from measured sections in the Lunpola Basin for zircon U-Pb dating (Figures 2 and 3; Text S2); two sandstone samples were collected from measured sections described by DeCelles et al. (2007a) in the Nima Basin. Seven modern sand samples were collected from mainstream riverbeds of several large rivers that terminate in the Lunpola-Silin Co-Nima area (Figure 1b; Table S1).

Accepted Article

© 2019 American Geophysical Union. All rights reserved.

4. Results and interpretations

4.1. Geochronology

Six tuffites were sampled from different sections in the Lunpola Basin (Figures 2 and 3). Crystal and vitric pyroclasts dominate the microstratified tuffites with interstitial materials of tephra, silt, and clay (Figure S2a). All tuffite samples yield Eocene to Miocene zircon U-Pb ages with more than 50% of measurements yielding ages <30 Ma (Figure 2a). These young zircons are euhedral, displaying well-developed prismatic crystal forms and clear oscillatory zoning (Figures 2b and S2b). We interpret the euhedral zircons as first-cycle zircons that originated from the adjacent coeval volcanic eruptions; hence, the age of the youngest population must be near the actual depositional ages of the sampled succession. In this study, YC1σ (2+) ages (weighted mean ages of two or more grain ages overlapping in age at 1σ, Dickinson and Gehrels, 2009) are adopted to constrain the maximum depositional ages of tuffites, which are 9.22±0.13 Ma (15H1-254U), 16.77±0.34 Ma (14H8-370U), 17.59±0.32 Ma (13H4U), 21.10±0.42 Ma (14H4-128U), 22.57±0.48 Ma (14H3-48U), and 35.31±0.93 Ma (ZP15U1) (Figure 2a; Table S2). Notably, four tuffite-bearing successions were previously assigned as Paleocene to Eocene in age (Ma et al., 2015), namely, sections 15H1, 14H8, 14H3, and 14H4 (Figure 1c). The YPP ages (youngest graphical detrital zircon age peak on age-probability plot, Dickinson and Gehrels, 2009) are used to constrain the maximum depositional ages of four sandstone samples that yield the youngest age clusters with Cenozoic ages, namely, 22.8 Ma (ZP03), 38.5 Ma (13H14), 23.9 Ma and 26.5 Ma (15H2) (Figure 2c), and sections ZP03 and 15H2 were also previously regarded as Paleocene to Eocene in age (Ma et al., 2015).

Accepted Article

© 2019 American Geophysical Union. All rights reserved.

4.2. Stratigraphy

Deposits of sections 13H5, 13H4, 13H2, and 12H1 are dominated by hundred-meter thick sequences of structureless dark gray to green argillaceous rocks (Figure 3a), including thin-bedded siltstones, mudstones, marlstones, and paper-thin oil shales with fossil fish (Figures 3a, S3a-3b, and S4a-4b). Sections ZP15, 14H4, 15H1, and ZP03 are dominated by 10-200 m thick sequences of mottled, yellow to reddish, laterally continuous, upward-fining and coarsening packages of conglomerates and sandstones (Figures 3a and S4c). Gravels from pebble to boulder matrix-supported conglomerates are angular to subangular, disorganized, and unstratified (Figure S3c). Clast-supported pebble conglomerates are well sorted with imbricated clasts. Planar and trough cross-bedded coarse- to fine-grained pebbly sandstones are intercalated with rippled siltstones (Figure S3d). Massive and laminated, rippled, and bioturbated argillaceous rocks with soft-sediment deformation structures dominate the upper part of these sections (Figures S3e-3f). Alternating argillaceous and coarse clastic rocks dominate the other eight sections (Figure 3a). Both upward-fining and upward-coarsening successions comprise interbedded conglomerates, sandstones, siltstones, marlstones, and mudstones (Figures S4d-4e). Conglomeratic beds are clast-supported with well-sorted, subrounded to rounded, imbricated gravels and occasionally sharp erosional surfaces underlain by red nodule-bearing paleosol (Figures S4f-4g). Planar and trough cross-beddings and ripples are common in the sandstones (Figures S3g-3h). Argillaceous rocks consist of massive and laminated siltstones, marlstones, mudstones, and shales with ripples, rootlets, burrows, mud cracks, rain drops, slumps, and water escape structures (Figures S3i-3j). Laterally traceable laminated dolomitic limestones are occasionally present (Figure S4h).

The hundred-meter thick sequences of dark argillaceous rocks intercalated with fine-grained sandstones are interpreted as lacustrine deposits (Ma et al., 2015) (Figures 3a and S1). Dark gray, oil-rich shales with interbedded marlstones and siltstones suggest a semi-deep

© 2019 American Geophysical Union. All rights reserved.

Accepted Article

or deep lake environment (Wang et al., 2011b). Well-sorted, clast-supported conglomerates with wave rippled siltstones, and bioturbated mudstones indicate lake margin settings (Wei et al., 2017). The sequences of conglomerates and coarse- to fine-grained sandstones suggest pulses of coarse deltaic sedimentation (Wei et al., 2017). Subaqueous deltaic environments are evidenced by interbedded siltstones, marlstones, and mudstones, which contain rootlets, burrows, and soft-sediment deformation (DeCelles et al., 2007a; Wei et al., 2017). Braided river deposits are recorded by channelized, cross-bedded sandstones and erosive conglomerates with interbedded cross-bedded sandstones, and cross-laminated siltstones and mudstones (Wei et al., 2017). These facies are intercalated with nodular red-beds with desiccation cracks recording paleosols (DeCelles et al., 2007a). Matrix-supported conglomerates suggest debris flows possibly sourced from a nearby alluvial fan (DeCelles et al., 2007a). We interpret the depositional environments represented by these sections as being dominated by braided river channels and associated floodplains feeding fluvial-deltaic and lacustrine settings with proximal alluvial fans near the source areas. By combining these interpretations with the above age constraints, we correlate these sections and re-establish a stratigraphic framework from the late Eocene to late Miocene (ca. 35-9 Ma), and demonstrate that large and stable fluvio-lacustrine systems were present in the Lunpola area probably throughout most of the Miocene (ca. 23-9 Ma) (Figure 3a).

4.3. Provenance

Paleocurrent directions measured from cross-bedding, current ripple lamination, and imbricated gravels are highly variable but indicate a component of eastward to southward paleoflow with a small component of northward-directed flow (Figures 1c and 3a). Conglomerate compositions of measured sections are enriched in gray bioclastic and micritic limestones, red and green cherts, quartz, grayish-green and reddish sandstones, basalt, and

Accepted Article

© 2019 American Geophysical Union. All rights reserved.

andesite (Figure 3b). The modern rivers have comparable clast compositions and grain sizes in the main channels (Figures 3b-3c).

Jurassic to Lower Cretaceous marine strata in the southern Qiangtang and northern Lhasa terranes account for the presence of abundant bioclastic and micritic limestone clasts (Ma et al., 2017). Mélanges within the Bangong-Nujiang suture contributed the red and green cherts and basalt clasts (Ma et al., 2018). The reddish sandstone clasts were probably derived from the Upper Cretaceous red bed unit, which is predominant in the southern Qiangtang terrane (Meng et al., 2018). The andesite clasts were likely derived from the Lower Cretaceous volcanic unit, which is exposed to the north and south of the basin (Zhang et al., 2004). Sandstone petrology plots indicate that the sediments are mainly of a "recycled orogeny" source, with a fraction of the samples showing a "magmatic arc" source (Figures 3d and S5; Dickinson and Suczek, 1979), which refers to the strongly deformed Mesozoic strata and igneous rocks of central Tibet.

In total, 1116 zircon U-Pb concordant ages were obtained from the Lunpola Basin, 575 concordant ages from the modern river sands, and 197 measurements from the Nima Basin; the age spectra were plotted by integrating results presented by DeCelles et al. (2007a) (Figure 3e). The Cenozoic age population of 62-10 Ma in the Lunpola Basin is mainly from the newly dated tuffites. Fifteen Cenozoic ages present in the Nima Basin range from 64-34 Ma (Figure 3e). Middle Eocene to late Miocene (45-9 Ma) postcollisional volcanism in the Qiangtang terrane and the western Lhasa terrane could account for the presence of middle to late Cenozoic ages (Liu et al., 2017). The pre-Cenozoic ages of these two basins exhibit distinct clusters of 125-100 Ma, 620-250 Ma, 1160-720 Ma, 1950-1700 Ma, and 2630-2360 Ma, which are also evident in the pre-Cenozoic detrital zircon samples from the Qiangtang and Lhasa terranes (Figure 3e). The age distributions of river sands are highly similar to the

Accepted Article

© 2019 American Geophysical Union. All rights reserved.

ancient drainage basins (Figure 3e). Widespread Cretaceous igneous rocks in central Tibet are responsible for the prominent clusters of 125-100 Ma ages (Figure 1b).

5. Discussion and conclusions

The Cenozoic stratigraphic framework of the Lunpola Basin was previously established mainly as a result of hydrocarbon exploration in the region (Xu, 1980), and >5 km thick continental deposits can be observed in seismic profiles (Wu et al., 2016). Our newly established stratigraphic framework constrains up to ~2 km thick deposits within the basin (Figure 3a), which represent the uppermost part of the Cenozoic deposits. Therefore, most of the lower Cenozoic strata are still buried, so the new chronological constraints for the upper successions are significant for reinterpreting previous geophysical and borehole data and understanding the sedimentary response to surface and deep processes.

The representative zircon U-Pb age signals of the Qiangtang Central Uplift (240-200 Ma), Amdo microterrane (190-160 Ma), and southwestern Qiangtang terrane (160-140 Ma) are not detected in neither ancient nor modern drainage (Chapman and Kapp, 2017), indicating that the river networks of the Lunpola-Silin Co-Nima area have not drained these regions since the late Eocene. Typical age signals of the Linzizong volcanism (65-45 Ma) (Yin and Harrison, 2000) in the Gangdese mountains are not observed in the ancient drainage, whereas strong signals are present in the contemporaneous sediments accumulated in southern Tibet (DeCelles et al., 2011, 2014, 2016). Organic geochemistry studies indicate that the Miocene lakes in the Lunpola and Nima Basins were hypersaline (Wang et al., 2011a, 2011b), similar to the modern Silin Co Lake. Ma et al. (2015b) interpreted the Miocene Lunpola Lake as a balance-fill lake (Carroll and Bohacs, 1999), combined with the paleocurrent directions, we conclude that the Lunpola Basin has already been hydrologically closed since then. Integrating these data with the paleogeographic reconstruction of the Nima Basin presented by DeCelles et al. (2007a), we demonstrate that during the late Eocene to late

© 2019 American Geophysical Union. All rights reserved.

Accepted Article

Miocene, the internally drained Lunpola-Silin Co-Nima area was confined by the Tanggula Shan-Qiangtang Central Uplift to the north and the Gangdese mountains to the south, which also bound the proto-Tibetan Plateau (Wang et al., 2008). The rivers terminated in deltaic deposits on the edge of large saline lakes much as they do today (Figure 4). Facies and provenance analyses reveal that the Miocene large and stable fluvio-lacustrine systems with similar source regions (Figures 1b and 4a) and grain-size distributions to the modern system, which indicates that the ancient and modern drainages probably have similar hydrodynamic conditions. The sediment dispersal patterns and depositional environments are sensitive to the regional topographic relief and climate changes (Blum and Tornqvist, 2000; Dalrymple, 2010; Miall, 1977), and our results reveal that they are likely to have been persistent in central Tibet since the early Miocene. Besides, central Tibet has been suggested to have been in an arid and cold climate since the Oligocene (DeCelles et al., 2007b) and low erosion rates since the Eocene (Rohrmann et al., 2012). Thus, we propose that the low topographic relief has not changed significantly at least since the large and stable fluvio-lacustrine systems formed in the early Miocene.

Seismic observations and numerical modeling suggested that lower crustal flow and mantle processes were the main controlling mechanisms that caused flattening of the plateau surface (Bird, 1991; McKenzie and Jackson, 2002; Shen et al., 2001). However, the development of internal drainage was essential to developing the low-gradient landscape by aggradation and sediment redistribution (Liu-Zeng et al., 2008; Meyer et al., 1998). While central Tibet was internally drained, western Tibet was externally drained, and fluvial incision led to the present strong regional relief (Gourbet et al., 2016). The deceleration of erosion rates in central Tibet since the mid-Eocene (Hetzel et al., 2011) most likely implies a reduction in river incision, followed by sedimentation, which implies the initiation of internal drainage. The inability of rivers to flow out of the surrounding highlands and their connection

© 2019 American Geophysical Union. All rights reserved.

to a constant base level is required to maintain a long-standing internal drainage network (Sobel et al., 2003). As topographic growth of the Himalaya resulted in enhanced aridification in central Tibet, the ability of rivers to incise through surrounding mountains was reduced (Dupont-Nivet et al., 2007; Ramstein et al., 1997; Sobel et al., 2003), thus facilitating the development of internal drainage. Under such hydraulic and climatic conditions, many endorheic basins were formed in central Tibet with anoxic and saline water bodies (Han et al., 2014; Horton, 2012; Ma et al., 2015a, 2018). Ponding of the fluvial base level resulted in the lowering of hillslope gradients through weathering, erosion, and increased sediment aggradation; these processes combined to reduce overall gradients and thus define a plateau morphology. We conclude that central Tibet has been internally drained since at least the late Eocene; this geomorphic isolation enabled millions of years aggradation of fluvial systems and consequent diffusive lowering of hillslopes, resulting in the development of the relatively low-relief landscape no later than the early Miocene (Figure 4b).

The well-established stratigraphic framework provides a spatial-temporal constraint for basin evolution and its possible response to deeper geological processes (DeCelles et al., 2015). As a balance-fill lake (Ma et al., 2015b), the ancient Lunpola Lake subsided sufficiently to accommodate water and sediment fill (Carroll and Bohacs, 1999). The Lunpola Basin was suggested to have been a flexural basin bounded by steep, basement-involved thrust faults (Horton, 2012; Leeder et al., 1988) or, a rift basin in a transpressional setting (Schneider et al., 2003). The significant N-S thrusting in central Tibet, which was regarded as the primary control mechanism of the basin formation (Horton, 2012; Wei et al., 2017), ceased before ~23 Ma (Kapp et al., 2007) and hence predates the main phase of basin formation. Thus, the post-Oligocene basin evolution requires another suitable mechanism.

Accepted Article

© 2019 American Geophysical Union. All rights reserved.

The deformation pattern of central Tibet substantially changed from compression to extension (Li et al., 2015). Subsequently, central Tibet has been dominated by N-S extensional structures and V-shaped conjugate strike-slip faults, which have been suggested that facilitate the presence of topographic lowlands along the Bangong-Nujiang suture zone (Taylor et al., 2003). The E-W extension in central Tibet was proposed to have initiated in the early to middle Miocene (18-13 Ma) (Li et al., 2015), or even to have occurred concurrently with the N-S shortening after the Eocene (ca. 47 Ma) (Wang et al., 2010). The modern rivers flow dominantly westward over the site of the ancient lake into Silin Co (Figure 1b), and the E-W extension and strike-slip faulting likely account for the diversion of the river network and the relocation of the lake center. A deep seismic reflection profile reveals that the Moho depth is approximately 5-6 km deeper beneath the Bangong-Nujiang suture than beneath the southern Qiangtang and northern Lhasa terranes (Gao et al., 2013), which has been interpreted to result from ramp faulting in deep crust (Wu et al., 2016), and this thickness difference is slightly greater than those of the Cenozoic deposits in the Lunpola-Silin Co-Nima area. A paired general-shear model was suggested by Yin and Taylor (2011) as the mechanism for the formation of V-shaped conjugate strike-slip faults, which are attributed to the asthenosphere flow and eastward spreading of the thickened Tibetan lithosphere. DeCelles et al. (2015) and Wang et al. (2015) suggested that delamination or dripping of the lithosphere could have exerted a significant influence on basin subsidence in the central Andes, which also features high and broad internally drained hinterland and thickened crust, and this probably also occurred in the late Cenozoic Tibetan hinterland (Kapp and DeCelles, 2019). Taken all the above-mentioned events into account, we suggest that deep processes across the Bangong-Nujiang suture, such as lower crustal flow and/or even processes in the mantle lithosphere and asthenosphere, are likely coupled with the surface topography, basin subsidence and sedimentation (Gao et al., 2013; Wu et al., 2016; Yin and Taylor, 2011).

© 2019 American Geophysical Union. All rights reserved.

Accepted Article

Deep geological processes may not have been required to form the low-relief landscape, but it is reasonable to suggest that subsidence of these lake-filled basins along the Bangong-Nujiang suture responded to deep crustal or mantle flow. This speculation is supported by the latest 3-D simulations presented by Bischoff and Flesch (2018), which suggest that the flow of a weak lower crust could have led to surface subsidence in central Tibet.

Acknowledgments

The data supporting the conclusions can be obtained in the supporting information. This work was financially supported by the National Key R&D Plan (2017YFC0601405), Strategic Priority Research Program of CAS (XDA20070303), National Natural Science Foundation of China (41802124), and Key Laboratory of Sedimentary Basin and Oil and Gas Resources, Ministry of Natural Resources of the PRC (cdcgs2018006).

References

Andersen, T. (2002), Correction of common lead in U–Pb analyses that do not report 204Pb, *Chem. Geol.* , *192*(1–2), 59-79.

Bird, P. (1991), Lateral Extrusion of Lower Crust from under High Topography, in the Isostatic Limit, *Journal of Geophysical Research-Solid Earth and Planets*, *96*(B6), 10275-10286.

Bischoff, S. H., and L. M. Flesch (2018), Normal faulting and viscous buckling in the Tibetan Plateau induced by a weak lower crust, *Nature Communications*, *9*(1), 4952.

Black, L., and B. Gulson (1978), The age of the Mud Tank carbonatite, Strangways range, Northern Territory, *BMR Journal of Australian Geology and Geophysics*, *3*(3), 227-232.

Blum, M. D., and T. E. Tornqvist (2000), Fluvial responses to climate and sea-level change: a review and look forward, *Sedimentology*, *47*, 2-48.

Carroll, A. R., and K. M. Bohacs (1999), Stratigraphic classification of ancient lakes:

© 2019 American Geophysical Union. All rights reserved.

Accepted Article

Balancing tectonic and climatic controls, *Geology*, *27*(2), 99-102.

Chapman, J. B., and P. Kapp (2017), Tibetan Magmatism Database, *Geochemistry Geophysics Geosystems*, *18*(11), 4229-4234.

Chen, Y. L., G. R. Chen, K. Z. Zhang, and S. R. Zhao (2003), Report of 1:250,000 regional geological survey in Bange County.*Rep.*, Institute of Tibetan Geological Survey.

Clark, M. K., and L. H. Royden (2000), Topographic ooze: Building the eastern margin of Tibet by lower crustal flow, *Geology*, *28*(8), 703-706.

Dalrymple, R. D. (2010), Introduction to Siliciclastic Facies Models, in *Facies Models 4*, edited by N. P. James and R. W. Dalrymple, pp. 59-72, Geological Association of Canada, Canada.

DeCelles, P. G., P. Kapp, L. Ding, and G. E. Gehrels (2007a), Late Cretaceous to middle Tertiary basin evolution in the central Tibetan Plateau: Changing environments in response to tectonic partitioning, aridification, and regional elevation gain, *Geol. Soc. Am. Bull.* , *119*(5-6), 654-680.

DeCelles, P. G., P. Kapp, J. Quade, and G. E. Gehrels (2011), Oligocene–Miocene Kailas basin, southwestern Tibet: Record of postcollisional upper-plate extension in the Indus-Yarlung suture zone, *Geol. Soc. Am. Bull.* , *123*(7-8), 1337-1362.

DeCelles, P. G., P. Kapp, G. E. Gehrels, and L. Ding (2014), Paleocene-Eocene foreland basin evolution in the Himalaya of southern Tibet and Nepal: Implications for the age of initial India-Asia collision, *Tectonics*, *33*(5), 824-849.

DeCelles, P. G., J. Quade, P. Kapp, M. Fan, D. L. Dettman, and L. Ding (2007b), High and dry in central Tibet during the Late Oligocene, *Earth Planet. Sci. Lett.* , *253*(3-4), 389-401.

DeCelles, P. G., B. Carrapa, B. K. Horton, J. McNabb, G. E. Gehrels, and J. Boyd (2015), The Miocene Arizaro Basin, central Andean hinterland: Response to partial lithosphere

Accepted Article

© 2019 American Geophysical Union. All rights reserved.

removal?, *Geological Society of America Memoirs*, *212*, 359-386.

Decelles, P. G., I. S. Castañeda, B. Carrapa, J. Liu, J. Quade, R. Leary, and L. Zhang (2016), Oligocene‐Miocene Great Lakes in the India‐Asia Collision Zone, *Basin Research*.

Deng, T., S. Q. Wang, G. P. Xie, Q. Li, S. K. Hou, and B. Y. Sun (2012), A mammalian fossil from the Dingqing Formation in the Lunpola Basin, northern Tibet, and its relevance to age and paleo-altimetry, *Chin. Sci. Bull.* , *57*(2-3), 261-269.

Dickinson, W. R., and C. A. Suczek (1979), Plate tectonics and sandstone compositions, *AAPG Bull.* , *63*(12), 2164-2182.

Dickinson, W. R., and G. E. Gehrels (2009), Use of U–Pb ages of detrital zircons to infer maximum depositional ages of strata: A test against a Colorado Plateau Mesozoic database, *Earth Planet. Sci. Lett.* , *288*(1–2), 115-125.

Ding, L., P. Kapp, Y. H. Yue, and Q. Z. Lai (2007), Postcollisional calc-alkaline lavas and xenoliths from the southern Qiangtang terrane, central Tibet, *Earth Planet. Sci. Lett.* , *254*(1-2), 28-38.

Dupont-Nivet, G., W. Krijgsman, C. G. Langereis, H. A. Abels, S. Dai, and X. M. Fang (2007), Tibetan plateau aridification linked to global cooling at the Eocene-Oligocene transition, *Nature*, *445*(7128), 635-638.

Fan, J. J., C. Li, C. M. Xie, and Y. M. Liu (2016), Depositional environment and provenance of the upper Permian-Lower Triassic Tianquanshan Formation, northern Tibet: implications for the Palaeozoic evolution of the Southern Qiangtang, Lhasa, and Himalayan terranes in the Tibetan Plateau, *Int. Geol. Rev.*, *58*(2), 228-245.

Fielding, E., B. Isacks, M. Barazangi, and C. Duncan (1994), How flat is Tibet?, *Geology*, *22*(2), 163-167.

Gao, R., C. Chen, Z. W. Lu, L. D. Brown, X. S. Xiong, W. H. Li, and G. Deng (2013), New constraints on crustal structure and Moho topography in Central Tibet revealed by

Accepted Article

© 2019 American Geophysical Union. All rights reserved.

SinoProbe deep seismic reflection profiling, *Tectonophysics*, *606*, 160-170.

Gehrels, G., et al. (2011), Detrital zircon geochronology of pre-Tertiary strata in the Tibetan-Himalayan orogen, *Tectonics*, *30*(5).

Gourbet, L., G. Maheo, D. L. Shuster, A. Tripathy-Lang, P. H. Leloup, and J. L. Paquette (2016), River network evolution as a major control for orogenic exhumation: Case study from the western Tibetan plateau, *Earth Planet. Sci. Lett.* , *456*, 168-181.

Guynn, J., P. Kapp, G. E. Gehrels, and L. Ding (2012), U-Pb geochronology of basement rocks in central Tibet and paleogeographic implications, *J. Asian Earth Sci.* , *43*(1), 23-50.

He, H. Y., J. M. Sun, Q. L. Li, and R. X. Zhu (2012), New age determination of the Cenozoic Lunpola basin, central Tibet, *Geol. Mag.* , *149*(1), 141-145.

Hetzel, R., I. Dunkl, V. Haider, M. Strobl, H. von Eynatten, L. Ding, and D. Frei (2011), Peneplain formation in southern Tibet predates the India-Asia collision and plateau uplift, *Geology*, *39*(10), 983-986.

Horton, B. K. (2012), Cenozoic evolution of hinterland basins in the Andes and Tibet, in *Tectonics of Sedimentary Basins: Recent Advance*, edited by C. Busby and A. Azor, pp. 427-444, John Wiley & Sons, Oxford.

Hu, Z., W. Zhang, Y. Liu, S. Gao, M. Li, K. Zong, H. Chen, and S. Hu (2015), "Wave" Signal-Smoothing and Mercury-Removing Device for Laser Ablation Quadrupole and Multiple Collector ICPMS Analysis: Application to Lead Isotope Analysis, *Anal. Chem.* , *87*(2), 1152-1157.

Huang, T. T., J. F. Xu, J. L. Chen, J. B. Wu, and Y. C. Zeng (2017), Sedimentary record of Jurassic northward subduction of the Bangong-Nujiang Ocean: insights from detrital zircons, *Int. Geol. Rev.*, *59*(2), 166-184.

Ingersoll, R. V., T. F. Fullard, R. L. Ford, J. P. Grimm, J. D. Pickle, and S. W. Sares (1984),

© 2019 American Geophysical Union. All rights reserved.

Accepted Article

The effect of grain size on detrital modes; a test of the Gazzi-Dickinson point-counting method, *J. Sediment. Res.* , *54*(1), 103-116.

Jackson, S. E., N. J. Pearson, W. L. Griffin, and E. A. Belousova (2004), The application of laser ablation-inductively coupled plasma-mass spectrometry to in situ U-Pb zircon geochronology, *Chem. Geol.* , *211*(1-2), 47-69.

Kapp, P., and P. G. DeCelles (2019), Mesozoic–Cenozoic geological evolution of the Himalayan-Tibetan orogen and working tectonic hypotheses, *Am. J. Sci.* , *319*(3), 159-254.

Kapp, P., A. Yin, T. M. Harrison, and L. Ding (2005), Cretaceous-Tertiary shortening, basin development, and volcanism in central Tibet, *Geol. Soc. Am. Bull.* , *117*(7-8), 865-878.

Kapp, P., P. G. DeCelles, G. E. Gehrels, M. Heizier, and L. Ding (2007), Geological records of the Lhasa-Qiangtang and Indo-Asian collisions in the Nima area of central Tibet, *Geol. Soc. Am. Bull.* , *119*(7-8), 917-932.

Lai, W., X. M. Hu, D. C. Zhu, W. An, and A. L. Ma (2017), Discovery of the early Jurassic Gajia m,lange in the Bangong-Nujiang suture zone: Southward subduction of the Bangong-Nujiang Ocean?, *Int. J. Earth Sci.* , *106*(4), 1277-1288.

Leeder, M. R., A. B. Smith, and J. X. Yin (1988), Sedimentology, Paleoecology and Palaeoenvironmental Evolution of the 1985 Lhasa to Golmud Geotraverse, *Philosophical Transactions of the Royal Society a-Mathematical Physical and Engineering Sciences*, *327*(1594), 107-+.

Leier, A. L., P. Kapp, G. E. Gehrels, and P. G. DeCelles (2007), Detrital zircon geochronology of Carboniferous–Cretaceous strata in the Lhasa terrane, Southern Tibet, *Basin Research*, *19*(3), 361-378.

Leier, A. L., P. G. Decelles, P. Kapp, and G. E. Gehrels (2007), Lower Cretaceous Strata in the Lhasa Terrane, Tibet, with Implications for Understanding the Early Tectonic History

© 2019 American Geophysical Union. All rights reserved.

Accepted Article

of the Tibetan Plateau, *J. Sediment. Res.* , *77*(9-10), 809-825.

Li, G., M. Sandiford, X. Liu, Z. Xu, L. Wei, and H. Li (2014), Provenance of Late Triassic sediments in central Lhasa terrane, Tibet and its implication, *Gondwana Res.* , *25*(4), 1680-1689.

Li, S., C. Guilmette, L. Ding, Q. Xu, J.-J. Fu, and Y.-H. Yue (2017), Provenance of Mesozoic clastic rocks within the Bangong-Nujiang suture zone, central Tibet: Implications for the age of the initial Lhasa-Qiangtang collision, *J. Asian Earth Sci.* , *147*, 469-484.

Li, S., L. Ding, C. Guilmette, J. J. Fu, Q. Xu, Y. H. Yue, and R. Henrique-Pinto (2017), The subduction-accretion history of the Bangong-Nujiang Ocean: Constraints from provenance and geochronology of the Mesozoic strata near Gaize, central Tibet, *Tectonophysics*, *702*, 42-60.

Li, Y. L., C. S. Wang, J. G. Dai, G. Q. Xu, Y. L. Hou, and X. H. Li (2015), Propagation of the deformation and growth of the Tibetan-Himalayan orogen: A review, *Earth Sci. Rev.* , *143*, 36-61.

Liu-Zeng, J., P. Tapponnier, Y. Gaudemer, and L. Ding (2008), Quantifying landscape differences across the Tibetan plateau: Implications for topographic relief evolution, *Journal of Geophysical Research: Earth Surface*, *113*(F4).

Liu, D., Z. D. Zhao, D. J. DePaolo, D. C. Zhu, F. Y. Meng, Q. S. Shi, and Q. Wang (2017), Potassic volcanic rocks and adakitic intrusions in southern Tibet: Insights into mantle-crust interaction and mass transfer from Indian plate, *Lithos*, *268*, 48-64.

Liu, Y. S., S. Gao, Z. C. Hu, C. G. Gao, K. Q. Zong, and D. B. Wang (2010), Continental and Oceanic Crust Recycling-induced Melt-Peridotite Interactions in the Trans-North China Orogen: U-Pb Dating, Hf Isotopes and Trace Elements in Zircons from Mantle Xenoliths, *J. Petrol.* , *51*(1-2), 537-571.

Liu, Y. S., Z. C. Hu, S. Gao, D. Gunther, J. Xu, C. G. Gao, and H. H. Chen (2008), In situ

Accepted Article

© 2019 American Geophysical Union. All rights reserved.

analysis of major and trace elements of anhydrous minerals by LA-ICP-MS without applying an internal standard, *Chem. Geol.* , *257*(1-2), 34-43.

Ludwig, K. (2008), User's manual forisoplot 3.70, a geolocronological toolkit for Microsoft Excel, *Berkeley: Berkeley Geochronology Center Special Publication*, *4*, 25-32.

Ma, A., X. Hu, E. Garzanti, Z. Han, and W. Lai (2017), Sedimentary and tectonic evolution of the southern Qiangtang basin: implications for the Lhasa - Qiangtang collision timing, *Journal of Geophysical Research: Solid Earth*.

Ma, A. L., X. M. Hu, P. Kapp, Z. Han, W. Lai, and M. BouDagher-Fadel (2018), The disappearance of a Late Jurassic remnant sea in the southern Qiangtang Block (Shamuluo Formation, Najiangco area): Implications for the tectonic uplift of central Tibet, *Palaeogeography Palaeoclimatology Palaeoecology*, *506*, 30-47.

Ma, P. F., C. S. Wang, L. C. Wang, Y. L. Li, and J. Hu (2015a), Sedimentology and organic properties of lower Tertiary lacustrine source rocks, Lunpola Basin, central Tibetan Plateau: Implications for hydrocarbon potential, *Mar. Pet. Geol.* , *66*, 1029-1041.

Ma, P. F., L. C. Wang, C. S. Wang, X. H. Wu, and Y. S. Wei (2015b), Organic-matter accumulation of the lacustrine Lunpola oil shale, central Tibetan Plateau: Controlled by the paleoclimate, provenance, and drainage system, *Int. J. Coal Geol.* , *147*, 58-70.

Ma, P. F., Y. L. Li, C. S. Wang, L. Zheng, D. W. Lv, Y. Zou, and S. Li (2018), Oligocene-Miocene source rocks of the Zhongcang Basin: Implications for hydrocarbon potential differentiation between lake basins in Central Tibet, *Int. J. Coal Geol.* , *199*, 124-137.

Mao, Z., Q. Meng, X. Fang, T. Zhang, F. Wu, Y. Yang, W. Zhang, J. Zan, and M. Tan (2019), Recognition of tuffs in the middle-upper Dingqinghu Fm., Lunpola Basin, central Tibetan Plateau: Constraints on stratigraphic age and implications for paleoclimate, *Palaeogeogr. Palaeoclimatol. Palaeoecol.* , *525*, 44-56.

McKenzie, D., and J. Jackson (2002), Conditions for flow in the continental crust, *Tectonics*,

© 2019 American Geophysical Union. All rights reserved.

Accepted Article

21(6).

Meng, J., X. X. Zhao, C. S. Wang, H. Liu, Y. L. Li, Z. P. Han, T. Liu, and M. Wang (2018), Palaeomagnetism and detrital zircon U-Pb geochronology of Cretaceous redbeds from central Tibet and tectonic implications, *Geol. J.* , *53*(5), 2315-2333.

Meyer, B., P. Tapponnier, L. Bourjot, F. Metivier, Y. Gaudemer, G. Peltzer, G. Shunmin, and C. Zhitai (1998), Crustal thickening in Gansu-Qinghai, lithospheric mantle subduction, and oblique, strike-slip controlled growth of the Tibet plateau, *Geophys. J. Int.* , *135*(1), 1-47.

Miall, A. D. (1977), A review of the braided-river depositional environment, *Earth Sci. Rev.* , *13*(1), 1-62.

Pan, G. T., J. Ding, D. Yao, and L. Wang (2011), 1:1,500,000 Geological Map of Qinghai-Xizang Plateau and Adjacent Areas*Rep.*, China Geological Survey, Chengdu.

Pullen, A., P. Kapp, G. E. Gehrels, L. Ding, and Q. H. Zhang (2011), Metamorphic rocks in central Tibet: Lateral variations and implications for crustal structure, *Geol. Soc. Am. Bull.* , *123*(3-4), 585-600.

Pullen, A., P. Kapp, G. E. Gehrels, P. G. DeCelles, E. H. Brown, J. M. Fabijanic, and L. Ding (2008), Gangdese retroarc thrust belt and foreland basin deposits in the Damxung area, southern Tibet, *J. Asian Earth Sci.* , *33*(5-6), 323-336.

Qu, Y. G., Y. S. Wang, and J. X. Duan (2011), *Report of 1:250,000 regional geological survey in Duoba area.*, China University of Geosciences Press, Wuhan.

Ramstein, G., F. Fluteau, J. Besse, and S. Joussaume (1997), Effect of orogeny, plate motion and land sea distribution on Eurasian climate change over the past 30 million years, *Nature*, *386*(6627), 788-795.

Rohrmann, A., P. Kapp, B. Carrapa, P. W. Reiners, J. Guynn, L. Ding, and M. Heizler (2012), Thermochronologic evidence for plateau formation in central Tibet by 45 Ma, *Geology*,

© 2019 American Geophysical Union. All rights reserved.

Accepted Article

40(2), 187-190.

Royden, L. H., B. C. Burchfiel, and R. D. van der Hilst (2008), The geological evolution of the Tibetan plateau, *Science*, *321*(5892), 1054-1058.

Shen, F., L. H. Royden, and B. C. Burchfiel (2001), Large-scale crustal deformation of the Tibetan Plateau, *J. Geophys. Res. [Solid Earth] 106*(B4), 6793-6816.

Sobel, E. R., G. E. Hilley, and M. R. Strecker (2003), Formation of internally drained contractional basins by aridity-limited bedrock incision, *Journal of Geophysical Research-Solid Earth*, *108*(B7).

Sun, G. Y., X. M. Hu, H. D. Sinclair, M. K. BouDagher-Fadel, and J. G. Wang (2015), Late Cretaceous evolution of the Coqen Basin (Lhasa terrane) and implications for early topographic growth on the Tibetan Plateau, *Geol. Soc. Am. Bull.* , *127*(7-8), 1001-1020.

Sun, J. M., Q. H. Xu, W. M. Liu, Z. Q. Zhang, L. Xue, and P. Zhao (2014), Palynological evidence for the latest Oligocene-early Miocene paleoelevation estimate in the Lunpola Basin, central Tibet, *Palaeogeography Palaeoclimatology Palaeoecology*, *399*, 21-30.

Taylor, M., A. Yin, F. J. Ryerson, P. Kapp, and L. Ding (2003), Conjugate strike-slip faulting along the Bangong-Nujiang suture zone accommodates coeval east-west extension and north-south shortening in the interior of the Tibetan Plateau, *Tectonics*, *22*(4).

Vermeesch, P. (2012), On the visualisation of detrital age distributions, *Chem. Geol.* , *312*, 190-194.

Wang, C. S., X. X. Zhao, Z. F. Liu, P. C. Lippert, S. A. Graham, R. S. Coe, H. S. Yi, L. D. Zhu, S. Liu, and Y. L. Li (2008), Constraints on the early uplift history of the Tibetan Plateau, *PNAS 105*(13), 4987-4992.

Wang, H., C. A. Currie, and P. G. DeCelles (2015), Hinterland basin formation and gravitational instabilities in the central Andes: Constraints from gravity data and geodynamic models, in *Geodynamics of a Cordilleran Orogenic System: The Central*

© 2019 American Geophysical Union. All rights reserved.

Accepted Article

Andes of Argentina and Northern Chile, edited by P. G. DeCelles, M. N. Ducea, B. Carrapa and P. A. Kapp, Geological Society of America Memoir 212.

Wang, L. C., C. S. Wang, Y. L. Li, L. D. Zhu, and Y. S. Wei (2011a), Organic Geochemistry of Potential Source Rocks in the Tertiary Dingqinghu Formation, Nima Basin, Central Tibet, *J. Pet. Geol 34*(1), 67-85.

Wang, L. C., C. S. Wang, Y. L. Li, L. D. Zhu, and Y. S. Wei (2011b), Sedimentary and organic geochemical investigation of tertiary lacustrine oil shale in the central Tibetan plateau: palaeolimnological and palaeoclimatic significances, *Int. J. Coal Geol.* , *86*(2-3), 254-265.

Wang, Q., et al. (2010), Eocene north-south trending dikes in central Tibet: New constraints on the timing of east-west extension with implications for early plateau uplift?, *Earth Planet. Sci. Lett.* , *298*(1-2), 205-216.

Wang, Y. S., S. Q. Zhang, and Y. H. Xie (2012), *Report of 1:250,000 regional geological survey in Angdaercuo.*, China University of Geosciences Press, Wuhan.

Wei, W., Y. Lu, F. Xing, Z. Liu, L. Pan, and T. J. Algeo (2017), Sedimentary facies associations and sequence stratigraphy of source and reservoir rocks of the lacustrine Eocene Niubao Formation (Lunpola Basin, central Tibet), *Mar. Pet. Geol.* , *86*, 1273-1290.

Wu, Z., Q. Zhang, Y. Wu, and P. Ye (2016), Response of Sedimentary Depression to Crustal Thickening in the Silin Co Basin and Its Adjacent Areas,Tibet, *Acta Geol. Sin.*, *90*(9), 2181-2191.

Xia, D. X., and S. K. Liu (2008), *Stratigraphy (lithostratic) of Xizang Autonomous Region*, China University of Geosciences Press, Beijing.

Xu, Z. (1980), The tertiary and its petroleum potential in the Lunpola Basin, Tibet, *Oil & Gas Geology*, *1*(2), 153-158.

© 2019 American Geophysical Union. All rights reserved.

Accepted Article

Yin, A., and T. M. Harrison (2000), Geologic evolution of the Himalayan-Tibetan orogen, *Annu. Rev. Earth Planet. Sci.*, *28*, 211-280.

Yin, A., and M. H. Taylor (2011), Mechanics of V-shaped conjugate strike-slip faults and the corresponding continuum mode of continental deformation, *Geol. Soc. Am. Bull.* , *123*(9-10), 1798-1821.

Zhang, J. W., J. E. Dai, X. Y. Qian, Y. K. Ge, and C. S. Wang (2017), Sedimentology, provenance and geochronology of the Miocene Qiuwu Formation: Implication for the uplift history of Southern Tibet, *Geoscience Frontiers*, *8*(4), 823-839.

Zhang, K. J., B. D. Xia, G. M. Wang, Y. T. Li, and H. F. Ye (2004), Early Cretaceous stratigraphy, depositional environments, sandstone provenance, and tectonic setting of central Tibet, western China, *Geol. Soc. Am. Bull.* , *116*(9-10), 1202-1222.

Zhang, Q., L. Ding, F. Cai, X. Xu, L. Zhang, and Q. Xu (2011), Early Cretaceous Gangdese retroarc foreland basin evolution in the Selin Co basin, central Tibet: evidence from sedimentology and detrital zircon geochronology, *Geological Society, London, Special Publications*, *353*(1), 27-44.

Zhu, D. C., Z. D. Zhao, Y. L. Niu, Y. Dilek, and X. X. Mo (2011), Lhasa terrane in southern Tibet came from Australia, *Geology*, *39*(8), 727-730.

Accepted Article

© 2019 American Geophysical Union. All rights reserved.

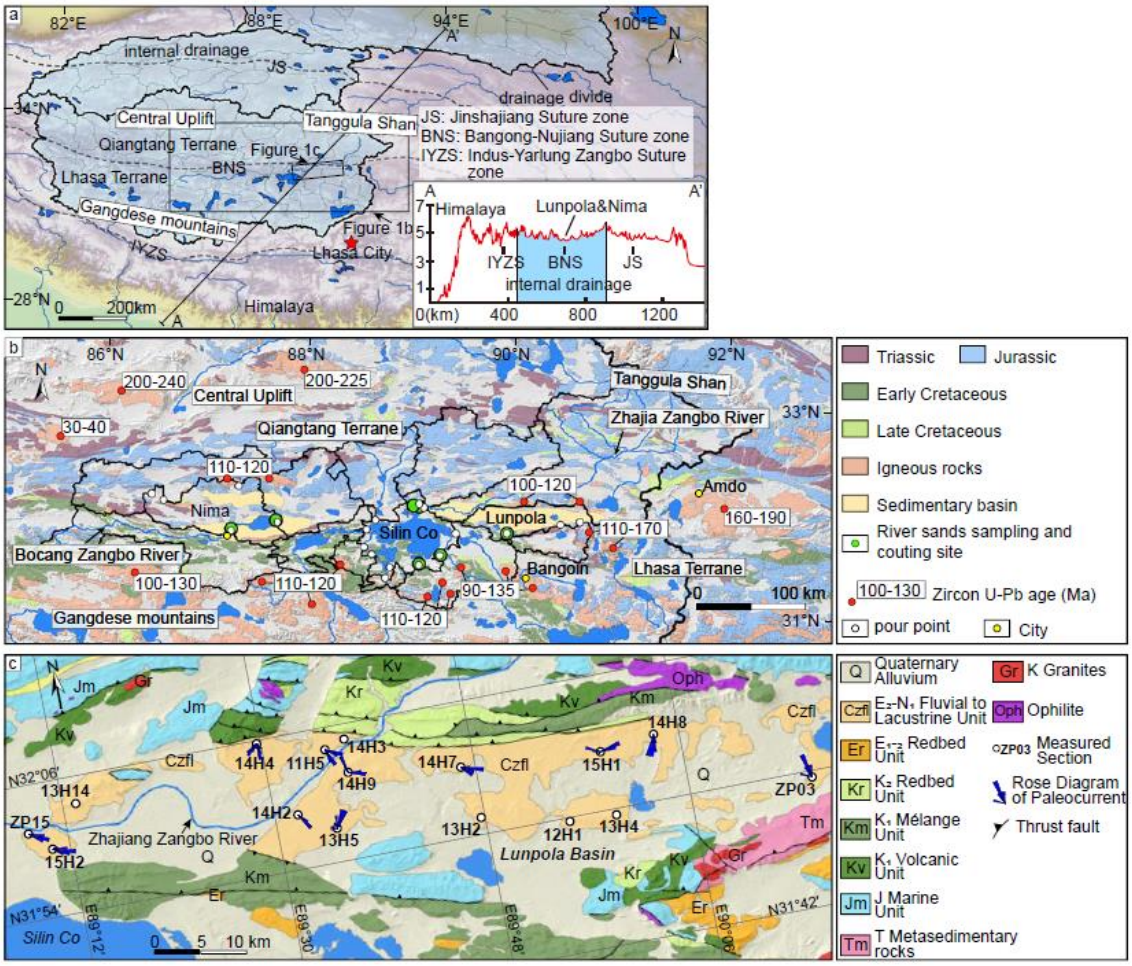

Figure 1. (a) Major geological features and modern internally drained basins (gray lines) of central Tibet. The light blue area is the internal drainage of the Tibetan Plateau. The insert is a topographic cross-section along line AA'. **(b)** Hillshade image of the Lunpola-Silin Co-Nima area with major catchments (black lines), Mesozoic strata and igneous rocks (adapted from Pan et al., 2011). **(c)** Geological map of Lunpola Basin (adapted from Chen et al., 2003; Qu et al., 2011; Wang et al., 2012).

Accepted

© 2019 American Geophysical Union. All rights reserved.

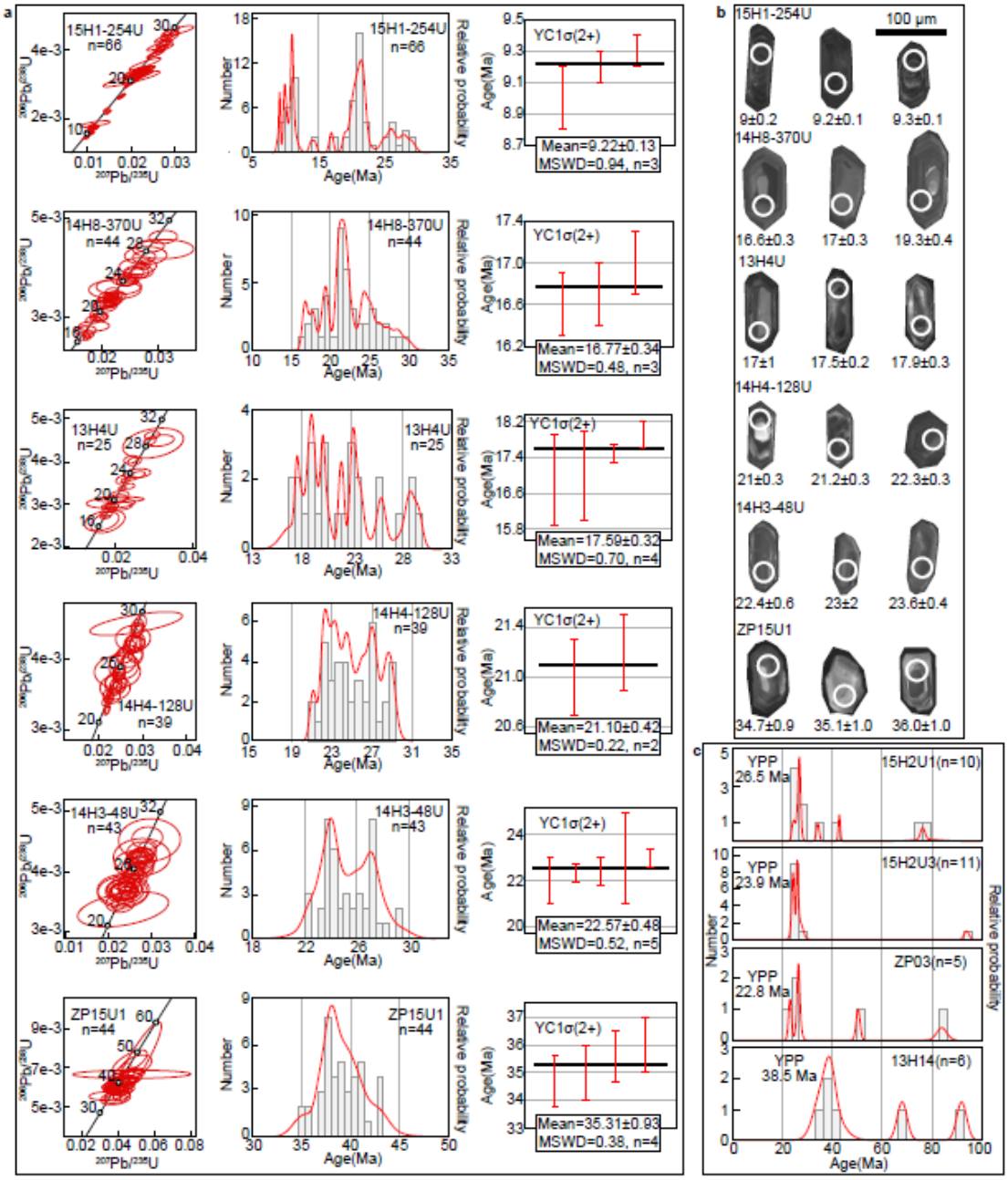

Figure 2. **(a)** Concordia plots (left column) and probability density diagrams (middle column) of <65 Ma zircons from tuffite samples; right column: YC1σ (2+) ages. **(b)** Selected cathodoluminescence images of dated zircons from tuffite samples. **(c)** Probability density diagrams of <100 Ma detrital zircons from four sandstone samples that show YPP ages.

© 2019 American Geophysical Union. All rights reserved.

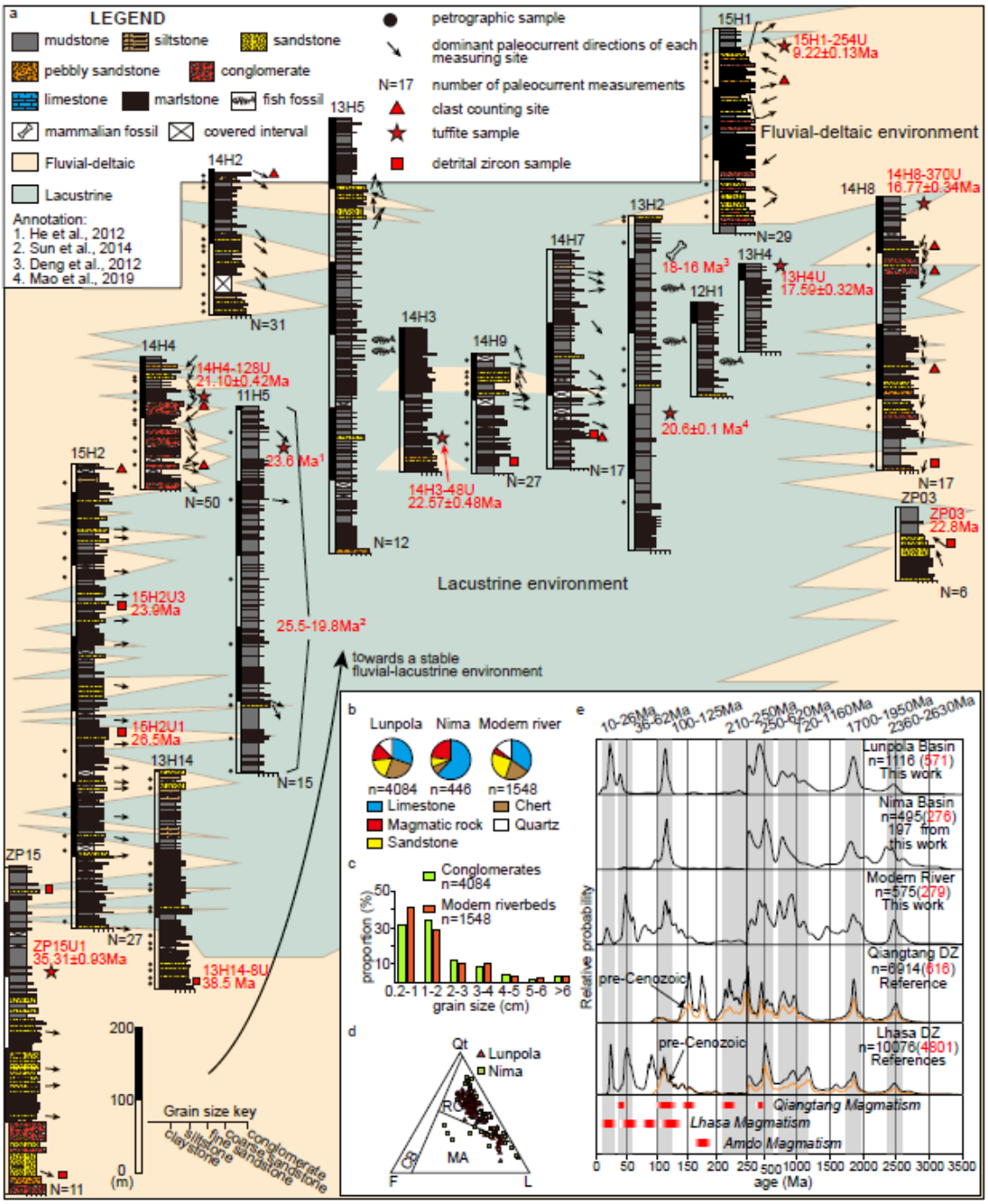

Figure 3. (a) Sedimentary logs of the measured sections. All the sections are correlated by zircon ages (YC1σ (2+) and YPP ages in red), published age constraints (annotation), fossil-bearing beds, facies analyses, and lateral correlation of outcrops. **(b)** Pie charts show conglomerate clast composition data from the Lunpola (this work) and Nima Basins (DeCelles et al., 2007a), and modern riverbeds (this work). n: counted grains. **(c)** Histograms

© 2019 American Geophysical Union. All rights reserved.

show the distribution of gravel grain sizes from conglomerate (from measured sections of the Lunpola Basin, see Figures 3a and S1 for the counting locations) and modern riverbeds (see Figure 1b for counting sites). **(d)** Ternary diagrams are showing how modal sandstone petrographic data from this work compare to coeval sediments in Nima Basin. Qt: total quartz; F: total feldspar; L: total lithic grains; CB: continental block, RO: recycled orogen, MA: magmatic arc. **(e)** Comparisons of kernel density estimation spectra of zircon U-Pb ages in this work and published data from modern rivers, Lunpola Basin, Nima Basin, Qiangtang terrane, and Lhasa terrane. Scale change at 250 Ma. n: number of analyses; bracketed red number is the number of grains with ages <250 Ma. Data sources: (Chapman and Kapp, 2017; DeCelles et al., 2007a; Fan et al., 2016; Gehrels et al., 2011, and references therein; Guynn et al., 2012; Huang et al., 2017; Lai et al., 2017; Leier et al., 2007a, 2007b; Li et al., 2014; Li et al., 2017a, 2017b, 2017c; Ma et al., 2017, 2018; Meng et al., 2018; Pullen et al., 2008, 2011; Sun et al., 2015; Zhang et al., 2017; Zhang et al., 2011; Zhu et al., 2011)

Accepted Article

© 2019 American Geophysical Union. All rights reserved.

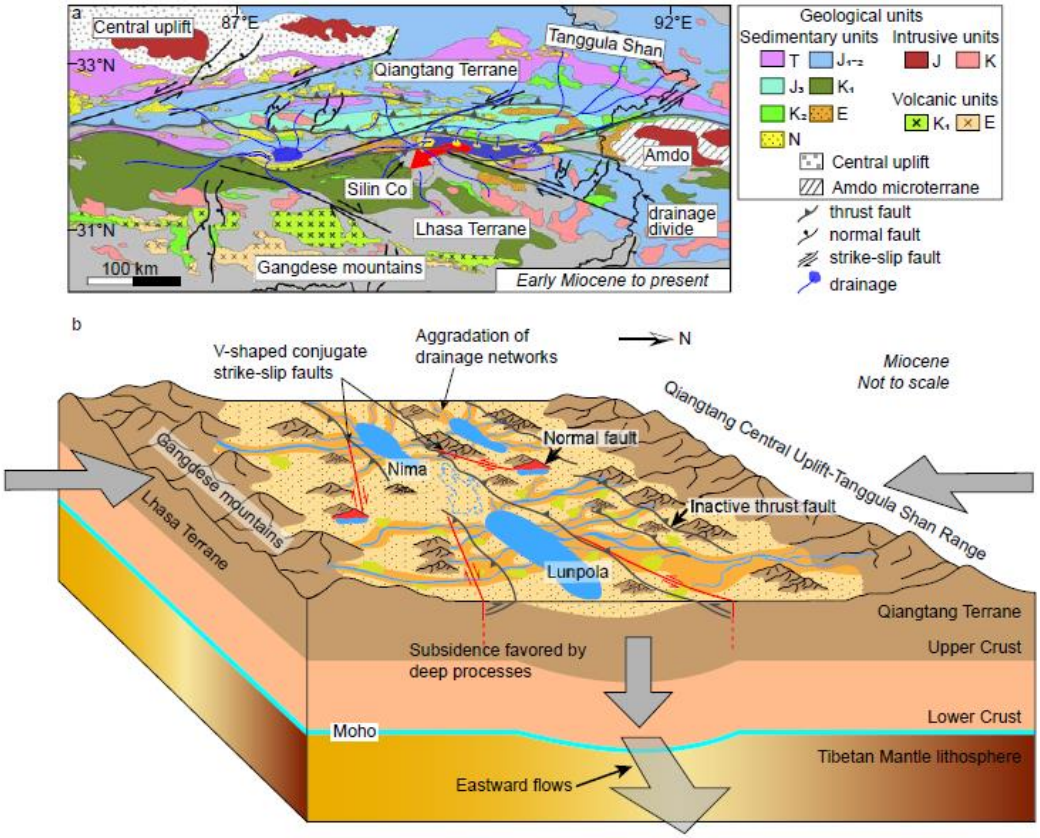

Figure 4. (a) Reconstruction of the paleodraiange. The dark gray area is pre-Mesozoic geological units that are not discussed in this work. **(b)** The schematic diagram for the drainage basin evolution and underlying deep processes. The schematic Moho morphology is adopted from Gao et al. (2013) and Wu et al. (2016). Thrust faults and conjugate strike-slip faults are after Wang et al. (2014) and Yin and Taylor (2011)

Accepted

© 2019 American Geophysical Union. All rights reserved.